FEBS Letters 589 (2015) 1883–1889

FEBS Letters

journal homepage: www.FEBSLetters.org

VirB6 and VirB10 from the *Brucella* type IV secretion system interact via the N-terminal periplasmic domain of VirB6

Ana Maria Villamil Giraldo [1], Charline Mary [1], Durgajini Sivanesan, Christian Baron *

Université de Montréal, Pavillon Roger-Gaudry, Department of Biochemistry and Molecular Medicine, C.P. 6128, Succ. Centre-Ville, Montréal, QC H3C 3J7, Canada

ARTICLE INFO

Article history:
Received 15 December 2014
Revised 27 May 2015
Accepted 27 May 2015
Available online 9 June 2015

Edited by Renee Tsolis

Keywords:
Type IV secretion system
Bacterial virulence
Protein–protein interaction
Membrane protein

ABSTRACT

Type IV secretion systems are multi-protein complexes that transfer macromolecules across the cell envelope of bacteria. Identifying the sites of interaction between the twelve proteins (VirB1–VirB11 and VirD4) that form these complexes is key to understanding their assembly and function. We have here used phage display, bacterial two-hybrid and fluorescence-based interaction assays to identify an N-terminal domain of the inner membrane protein VirB6 as a site of interaction with the envelope-spanning VirB10 protein. Our results are consistent with the notion that VirB6 acts in concert with VirB10 as well as with VirB8 during secretion system assembly and function.

1. Introduction

Type IV secretion systems (T4SS) are used by Gram-negative bacteria to transfer DNA and protein substrates across the cell envelope into target cells [1,2]. They usually consist of 12 proteins, VirB1–11 and VirD4, which assemble into a multi-protein channel that has anchoring points at both the inner and the outer membrane. The overall architecture was first determined for the outer part of the plasmid pKM101-T4SS using cryo-electron microscopy and X-ray crystallography and it was found to be composed of homologs of VirB7, VirB9 and the C-terminal domain of VirB10 [3,4]. Analysis of the cryo-electron microscopic structure of the plasmids R388 T4SS revealed the overall structure of the inner membrane part of the channel and showed the localization of VirB4 [5]. However, the exact topologies and the nature of the interactions between the proteins forming the inner membrane complex (VirB6, VirB8 and VirB10) remain unknown.

In this work, we have focused on the analysis of the interaction between VirB6 and VirB10. VirB6 is a polytopic inner membrane protein essential for substrate secretion. It is one of the channel subunits that is likely in direct contact with the DNA substrate during its transfer across the inner membrane [6]. The DNA transfer assays suggested that VirB6 acts in concert with VirB8 and we have provided direct evidence for this notion identifying a presumably periplasmic loop of VirB6 as site of interaction [7]. So far, no structural information is available for VirB6-like proteins, but the homologous proteins ComB6 from *Helicobacter pylori* and VirB6 from *Agrobacterium tumefaciens* have been characterized using biochemical and genetic approaches [8,9]. They are highly hydrophobic proteins, which contain five transmembrane segments and a large periplasmic loop located in their central region. The N-terminal domain of both VirB6 homologs is located in the periplasm.

VirB10 is another essential component of the T4SS and being anchored both to the inner and the outer membranes it spans the entire translocation channel. The crystal structure of the C-terminal domain of the VirB10 homolog TraF was characterized in the context of the outer membrane core complex formed by TraN–TraO–TraF (VirB7–VirB9–VirB10) [3]. According to this structure, the outer membrane channel is primarily formed by 14 copies of VirB10, which makes direct contacts with VirB9 and VirB7 in the external part of the channel. This architecture was surprising as the seminal studies using DNA immunoprecipitation had failed to show a direct contact between VirB10 and the translocated

Abbreviations: T4SS, type IV secretion systems; BTH, bacterial two-hybrid; AC, adenylate cyclase; FRET, fluorescence resonance energy transfer

Author contributions: Ana Maria Villamil Giraldo: conducted experiments and wrote manuscript; Charline Mary: conducted experiments; Durgajini Sivanesan: conducted experiments; Christian Baron: wrote and revised manuscript.

* Corresponding author.
E-mail address: christian.baron@umontreal.ca (C. Baron).
[1] These authors made equal contributions to this manuscript.

http://dx.doi.org/10.1016/j.febslet.2015.05.051

substrate [6]. The complex formed by the plasmid R388 T4SS homologs VirB3 to VirB10 was recently characterized by cryo-electron microscopy [5]. 24 copies of VirB6 and 14 copies of VirB10 were found to be forming part of the assembly. However, this analysis did not reveal the localization of VirB6 or the N-terminal domain of VirB10 within the inner membrane complex.

VirB6 and VirB10 have also been studied from a functional perspective. VirB6 is essential for substrate interactions and substrate transfer to other VirB proteins [8]. Transferring of substrate from VirB6 and VirB8 to VirB2 and VirB9 depends on VirB10 [6] and its efficiency is affected by the conformational change undergone by VirB10 upon ATP binding to the T4SS energizing proteins VirD4 and VirB11 [10]. Despite these data suggesting close functional links, no evidence was available for a direct interaction between VirB6 and VirB10. To address this question, we used a combination of biochemical and genetic interaction assays to identify specific VirB10-interacting regions within VirB6 from the model organism *Brucella*. Our results show that the N-terminal region of VirB6 interacts with VirB10. In combination with previous data from our group [7] these results suggest that VirB6 interacts simultaneously with VirB8 and with VirB10.

2. Materials and methods

2.1. Plasmid, strain constructions and mutagenesis

DNA manipulations followed standard procedures [11]. The strains and plasmids used are given in Table 1 (Supplementary information). *Escherichia coli* strains JM109 (DE3) and BL21 (DE3) were used as hosts for cloning and mutagenesis and protein overproduction, respectively.

2.2. Cultivation of bacteria

Cultures of *E. coli* JM109 for cloning experiments were grown at 37 °C in LB medium (1% tryptone, 0.5% yeast extract, 1% NaCl) in the presence of antibiotics for plasmid propagation (ampicillin [amp], 100 μg/ml; kanamycin [kan], 50 μg/ml). For protein overproduction, *E. coli* strain BL21star (λDE3) was grown under aerobic conditions at 37 °C in LB to exponential phase (optical density at 600 nm (OD_{600}) of 0.4–0.8), followed by the addition of 0.5 mM IPTG (isopropyl-β-D-thiogalactopyranoside) to induce gene expression. Cultivation under aerobic conditions proceeded at 26 °C for 16 h after induction.

2.3. Purification of fusion proteins

pHTvirB8sp, pHTvirB10sp (encoding periplasmic domains of *Brucella* VirB8 and VirB10) and their variants were transformed into BL21star (DE3) and protein overproduction and purification were carried out as described previously [12]. Briefly, bacterial cells were harvested, resuspended in binding buffer (50 mM sodium phosphate, 300 mM NaCl, 40 mM imidazole, pH 7.4) and lysed using a One Shot cell disrupter (Constant Systems Inc.) at 27 kPsi. Lysates were subsequently centrifuged twice at 13 000 rpm (4 °C), filtered through a 0.45 μm membrane, loaded onto a HisTrap Ni-chelate column (GE Healthcare) and eluted over a linear 50 ml gradient from 40 to 500 mM imidazole. Proteins were then concentrated, desalted into TEV buffer (25 mM sodium phosphate, 125 mM NaCl, 5 mM DTT, pH 7.4) and subjected to cleavage of the N-terminal His-tag using His-tagged TEV protease in a ratio of 1:70 for 15 h at 20 °C. The solution was diluted ten times, centrifuged at 13 000 rpm (4 °C), filtered through a 0.45 μm membrane and passed through a pre-equilibrated HisTrap Ni-chelate column. The flow through containing cleaved VirB8 or VirB10 was collected.

2.4. Determination of the localization of the VirB6 C-terminus

The gene encoding GFP was fused to the region of *virB6* encoding the C-terminus of the protein using the pWarf vector system and fluorescence emission (ʎ exc 485 nm ʎ em 512 nm) was measured as described [13]. The level of protein production was assessed by quantifying the intensities of the signals corresponding to the fusion proteins after performing a Western blot using anti-GFP antiserum (Roche).

2.5. Phage display

Purified VirB10 (100 μg/mL) in 0.1 M $NaHCO_3$ pH 8.6 was adsorbed onto polystyrene microtitre plates (Thermo Scientific) and incubated at 4 °C for 16 h, followed by incubation for 2 h at 37 °C with blocking buffer (0.1 M $NaHCO_3$, pH 8.6; 5 mg/ml BSA; 0.02% NaN_3). Phage libraries (Ph.D.-12 or Ph.D.-C7C) were diluted to 4×10^{10} pfu/ml from the original library (New England Biolabs, NEB), added to the plate, followed by washing with TBS-T and elution of VirB10-binding phage using 100 μl of elution buffer (0.2 M glycine–HCl, pH 2.1; 1 mg/ml BSA). Amplification of phage, phage separation and titering were performed as described previously [14]. Single-stranded DNAs were isolated from 1.5 ml of individually isolated plaque supernatant using the QIAprep M13 kit (Qiagen). Forward 1 (5′-GTGACGATCCCGCAAAAGCGGCCT-3′) and 96gIII primers (5′-CCCTCATAGTTATTAGCGTAACG-3′) were used to amplify the DNA sequence encoding the surface-exposed peptide. Each PCR product was sequenced to identify the encoded peptide sequence. Unique peptides were aligned to VirB6 sequence using Relic server's MATCH program which uses a default scoring window of 5 and a threshold score of 13 [15]. Pair-wise similarity is calculated for each scoring window of residues. We also used MatchScan (P.D. Pawelek, Concordia University, Montréal) that allows calculation of peptide similarity using a wide range of residue windows and scores.

2.6. SDS/PAGE and Western blotting

Cells and protein samples were incubated in Laemmli sample buffer for 5 min at 100 °C, followed by SDS–PAGE [16,17].

2.7. Bacterial two-hybrid assay (BTH)

Interactions between VirB6 variants and VirB10 were assessed in vivo using the BTH system [18]. The genes encoding VirB6 variants and full length VirB10 were fused to the DNA sequences encoding the T18 and T25 fragments of the catalytic domain of *Bordetella pertussis* adenylate cyclase (AC), and they were co-expressed in BTH101 AC (*cya*) deficient cells. The interaction was detected using the functional complementation between the two catalytic AC fragments leading to cAMP/β-galactosidase production detected using ortho-nitrophenyl-β-D-galactopyranoside as the substrate. The levels of protein production were assessed using Western blot analyses with anti-CyaA (3D1) antiserum (Santa Cruz Biotechnology Inc.).

2.8. Protein labeling

Conjugation reactions of Alexa Fluor 488 (A10254, Invitrogen) or Alexa Fluor 546 (A10258, Invitrogen) were performed according to the instructions of the manufacturer. Briefly, 10 μl of a freshly prepared aqueous solution of the dye (10 mg/ml) was added to previously reduced protein or peptide dissolved in 100 mM Tris–HCl pH 7.3, 150 mM NaCl and incubated in the dark for 2 h at room temperature. Excess probe was quenched by adding a 100-fold molar excess of dithiotreitol and removed using a Sephadex G-25

pre-packed Nap-5 column. The labeled product was further purified using a gel filtration Superdex 75 or Superdex Peptide column.

2.9. Fluorescence measurements

Fluorescence emission spectra were measured at room temperature in 100 mM Tris–HCl pH 7.3, 150 mM NaCl using a Cary Eclipse spectrofluorometer. Excitation wavelength was set to 488 nm and spectra were recorded between 500 and 600 nm. Fluorescence resonance energy transfer (FRET) was assessed by the decrease in Alexa fluor 488-labeled VirB10 fluorescence in the presence of Alexa fluor 546-labeled peptides and calculated as $1 - (F'/F)$ where F' and F are the donor emission in the presence and absence of the acceptor, respectively. K_D values were calculated according to Wang et al. [19]. The concentration of VirB10 was 3 μM. The fluorophore was chemically attached to an extra Cys residue inserted by mutating the gene at position 57 of VirB10. VirB10 contains two Cys residues, which in the homologous protein from *A. tumefaciens* were shown to form a disulfide bridge essential for protein function [20]. We therefore performed the labeling under conditions in which disulfide bonds are preserved. The synthetic VirB6-peptides included an extra Cys residue at their N-terminus used for covalent binding of the fluorophore and contained the following aminoacid sequences: IGTSIHNQLNNYVTMVASNTMNMI (peptide I), DAFAGNHGTPSSTIY QTLDNSLGKGWNIAAMLFEKGDNRGLT (peptide II), and TSIFSGSS GGGGSGSAKAGGESSYSAGGN (peptide III).

3. Results and discussion

3.1. Analysis of the topology of VirB6

It is generally accepted that the consensus among different methods makes the prediction of transmembrane segments more reliable [21]. We used five programs to predict the *Brucella* VirB6 transmembrane topology. All of them predicted seven transmembrane segments located in similar regions of the protein (Fig. 1). Interestingly, *Brucella* VirB6 (347 amino acids) is significantly longer than its homolog from *Agrobacterium* (295 amino acids). The functions of these additional amino acids are unknown, but the increased length of the hydrophobic portion explains why the presence of two additional transmembrane segments is predicted (seven vs five) and the overall predicted topology is very similar. One of the methods used (TMHMM) also predicts the orientation of the transmembrane segments [22] and according to this prediction the VirB6 C-terminus locates in the cytoplasm.

To experimentally determine the location of the C-terminus we performed a reporter assay in which GFP was C-terminally fused to VirB6. In addition, to assess the possibility of an alternative orientation, we used a control in which a protein fragment providing an extra transmembrane segment derived from glycophorin A was inserted between the VirB6 C-terminus and GFP (Fig. 2A) [13]. Normalized fluorescence of cells expressing GFP directly fused to the VirB6 C-terminus was much higher than that of cells carrying the alternative construct (Fig. 2B). Since GFP is fluorescent in the cytoplasm and non-fluorescent when directed to the periplasm, we conclude that VirB6 C-terminus locates inside the cytoplasm.

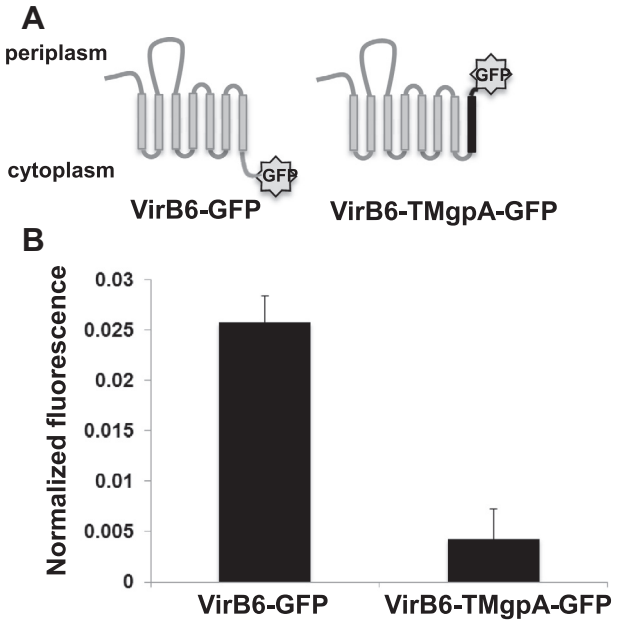

Fig. 2. Localization of VirB6 C-terminus. (A) The gene encoding VirB6 was cloned into pWarf(−) and pWarf(+) vectors. The resulting constructs code for VirB6 C-terminally fused to GFP (VirB6-GFP) and VirB6 C-terminally fused to GFP, preceded by a glycophorin transmembrane segment (VirB6-TMgpA-GFP). The predicted orientations of the two VirB6 fusions are shown (VirB6 transmembrane helices in gray, glycophorin transmembrane region in black, loops as black strokes); GFP is fluorescent only in the cytoplasm. (B) Fluorescence (excitation at 485 nm, emission at 512 nm) of whole cells expressing VirB6 fusions either in pWarf(−) or pWarf(+) relative to the value of optical density at 600 nm was normalized by the level of protein production assessed by Western blot with GFP-specific antibodies (not shown). Values and standard deviation were calculated from three independent experiments.

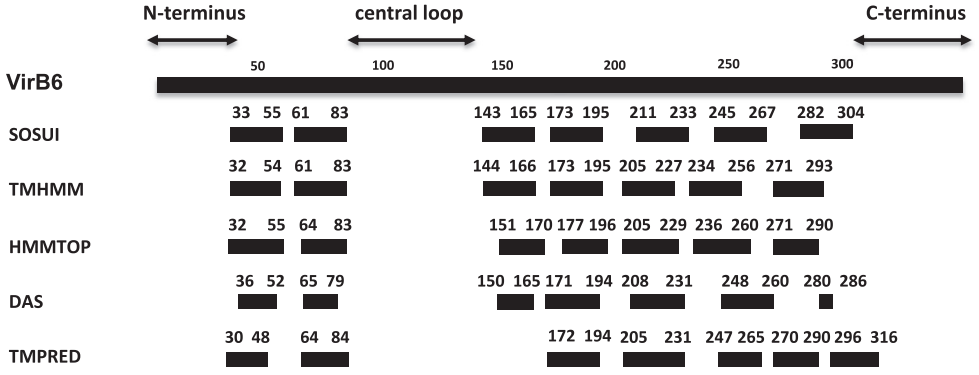

Fig. 1. Predicted topology of VirB6. Predicted transmembrane segments are shown as black rectangles with residue numbers relative to the N terminus. The N-terminus, the central loop region and the C-terminus are indicated. The five methods used are listed on the left: SOSUI: http://bp.nuap.nagoya-u.ac.jp/sosui/; TMHMM: www.cbs.dtu.dk/services/TMHMM/; HMMTOP: www.enzim.hu/hmmtop/; DAS: www.sbc.su.se/~miklos/DAS/; and TMpred: www.ch.embnet.org/software/TMPRED_form.html.

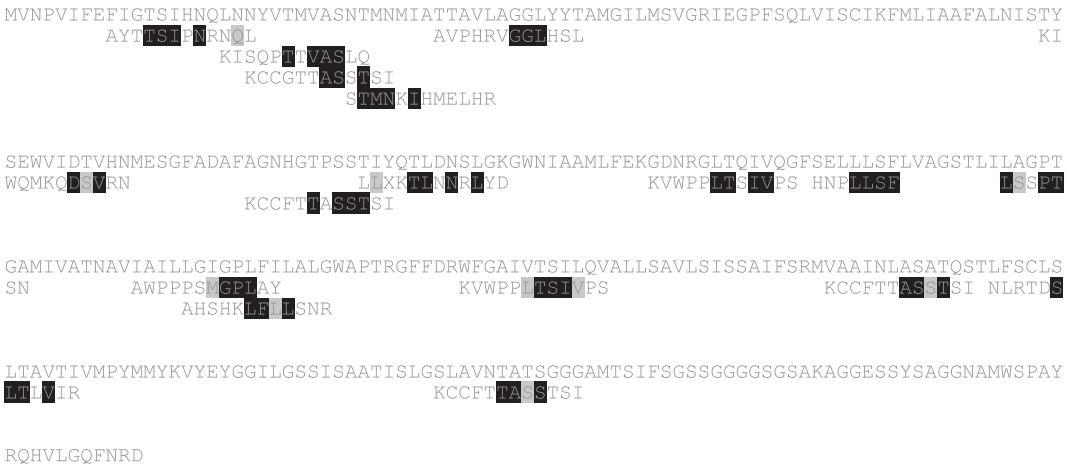

Fig. 3. Identification of VirB10 binding peptides by phage display. The purified periplasmic domain of VirB10 was subjected to three rounds of panning using the Ph.D.-C7C and Ph.D.-12 M13 phage display libraries. The sequences of the affinity-selected peptides were aligned to different regions of the VirB6 sequence using RELIC software [15]. Identical residues are highlighted in black and conserved residues are highlighted in gray.

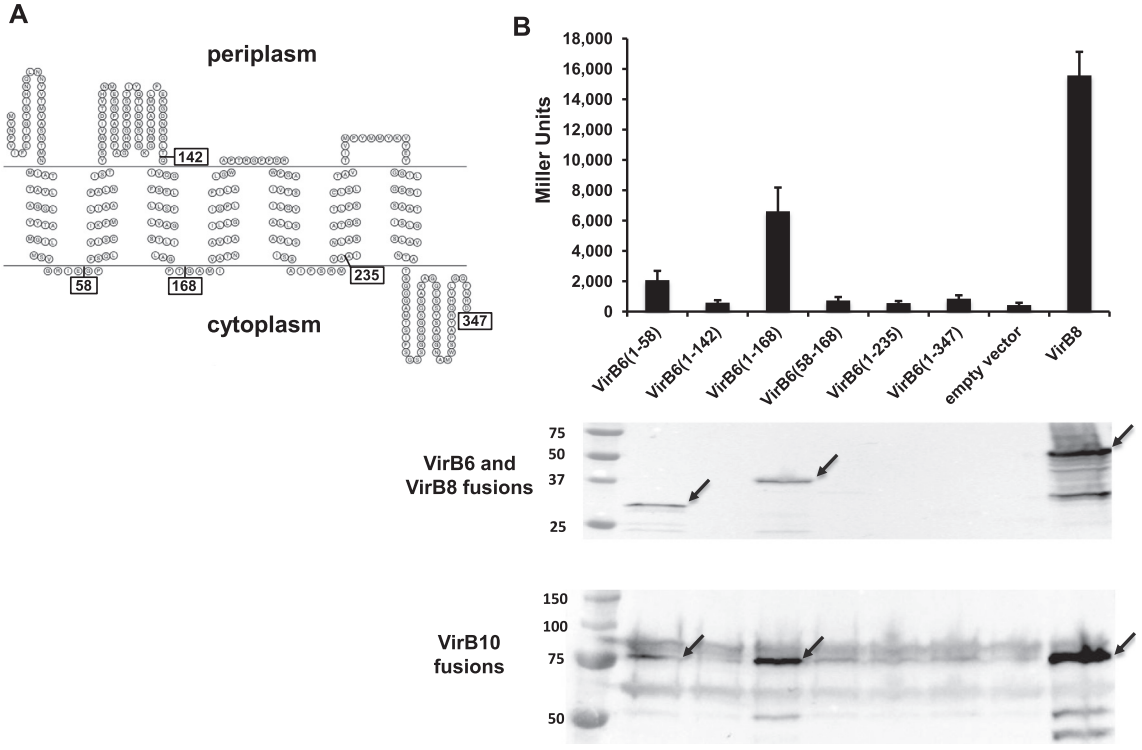

Fig. 4. In vivo analysis of VirB6 and VirB10 interactions using bacterial two hybrid assay. (A) Full length VirB10 and different domains of VirB6 (fusion after amino acids 58, 142, 168, 235 and 347 (full length) and after the region comprising amino acids 58–168) were expressed as fusions to the T25 and T18 domains of adenylate cyclase, respectively. (B) The interactions between VirB6 domains and VirB10 were assessed using the bacterial two-hybrid assay measuring β-galactosidase activity. The interaction between VirB10 and VirB8 [24] was used as the positive control while co-expression of the plasmid expressing T25VirB10 with an empty T18 fusion vector was used as the negative control. Values and standard deviations were calculated from three independent experiments. The lower panels show the Western blots using anti-Cya antibodies. Signals shown by arrows correspond to the predicted molecular masses of T18VirB6 1–58 fusion protein in the first lane, T18VirB6 1–168 in the third lane, and T18VirB8 in the last lane. The T25VirB10 fusion protein was equally detected at the predicted molecular mass in the strains expressing these three fusion proteins, signals of lower molecular masses likely correspond to degradation products.

These data, together with the consensus of the different computational methods predicting an uneven number of transmembrane segments, imply that the C-terminal region of VirB6 localizes in the cytoplasm and that the central loop locates in the periplasm, which is similar to the topology of Agrobacterium VirB6 [8]. This places the N-terminus and the central periplasmic loop in the same compartment as the periplasmic domains of possible interaction partners VirB8 and VirB10.

3.2. VirB10-interacting domains of VirB6 identified by phage display

To identify VirB10-interacting domains within VirB6 we used phage display, an unbiased approach aimed at identifying interacting regions using large randomized libraries of peptides displayed on the surface of phages [14,23]. The purified periplasmic domain of VirB10 was fixed on a plate and incubated with M13 phage libraries displaying random 12-mer peptides (Ph.D.-12 library) or

7-mer constrained peptides (Ph.D.-C7C library) on the surface of the M13 pIII protein. The binding phages were enriched by three rounds of panning. Sequencing of the DNA encoding the displayed peptides identified 125 unique peptides (Table 2, supplementary information). The sequences were aligned against VirB6 sequence using the RELIC server MATCH program [15]. As the phage display approach is a screening method based on fully randomized peptide libraries, the selected sequences were not expected to provide exact matches with interacting proteins. However, this approach identified several peptides with similarity to VirB6 that aligned with different regions of the protein, including the central periplasmic loop and the N-terminus (Fig. 3). We next tested these possible interaction sites using both in vivo and in vitro methods.

3.3. The VirB6 N-terminal domain interacts with VirB10 in vivo

The interaction between VirB10 and VirB6 was next assessed using the bacterial two-hybrid (BTH) system in which each protein was fused to the N- or the C-terminal domains of adenylate cyclase (AC), respectively. The readout of the assay consists of detecting β-galactosidase activity induced by the cAMP produced by the resulting enzymatic activity when the N- and C-terminal domains of AC are brought together by interacting fusion proteins. We co-expressed different fragments of VirB6 covering the potential interacting regions (Fig. 4A) fused to the C-terminus of CyaA with full-length VirB10 fused to the N-terminus of CyaA. VirB8, a known interaction partner of VirB10 was used as positive control and co-expression with empty fusion protein vectors were used as negative control. We detected β-galactosidase activity in strains expressing VirB6 residues 1–58 and 1–168 fused CyaA, but not in the case of fusion proteins to other fragments or to full-length VirB6 (Fig. 4B), suggesting that these regions interact with VirB10.

To determine whether β-galactosidase activities correlated with the accumulation of VirB6 fusion proteins in the cell, we conducted Western blot analysis to detect the CyaA portions of the fusion proteins. We detected VirB6 fusion proteins only in cells in which β-galactosidase activity was detected suggesting that the other fusion proteins may not be expressed or not be stable. Interestingly, the VirB10-CyaA fusion protein was also detected only in cells which β-galactosidase activity was detected, suggesting that VirB10 and its interacting domains from VirB6 as well as VirB8 mutually stabilize each other. Whereas the negative results with full-length VirB6 and other fusion proteins could be due to misfolding or low expression, the positive results in case of VirB6 1–58 and 1–168 fusions strongly suggest that this part of VirB6 contains a VirB10 binding site. In order to better define the region in VirB6 that interacts with VirB10, we next conducted in vitro FRET experiments with synthetic VirB6 peptides and the periplasmic domain of VirB10.

3.4. The VirB6 N-terminal domain interacts with VirB10 in vitro

Fluorescence resonance energy transfer (FRET) is a widely used method to analyze interactions between proteins. We used this approach to explore specific interactions between different VirB6-derived peptides and the periplasmic domain of VirB10. VirB6-derived synthetic peptides covering amino acids 10–33 (N-terminus, peptide I) and 100–143 (central periplasmic loop, peptide II) were chosen to represent potential interaction sites identified by phage display and the BTH assay. A third synthetic peptide comprising amino acids 301–329 (C-terminus, peptide III), which according to the predicted topology would be located in the cytoplasm, was used as a negative control. They were labeled via N-terminal Cys residues with acceptor fluorophore (Alexa fluor 456) and VirB10 was labeled with donor fluorophore (Alexa fluor 488). Fluorescence emission of donor-labeled VirB10 was measured upon increasing concentrations of acceptor-labeled VirB6 peptides. Addition of the peptide corresponding to the N-terminal domain of VirB6 increased FRET efficiency (reduced donor emission) with an apparent K_D value of ~4 μM while the peptides corresponding to the central periplasmic loop and the C-terminus did not impact donor emission (Fig. 5). These results agree with the results of the phage display and BTH assays suggesting that the N-terminal region comprises an interaction site with VirB10.

3.5. VirB6 peptides that interact with VirB10 or VirB8 do not disrupt the VirB8 and VirB10 interactions

Considering that the N-terminal peptide interacts with VirB10, the central VirB6 peptide interacts with VirB8 [7] and that VirB8 also interacts with VirB10 [24], we reasoned that these interactions may impact each other. To test this possibility, we conducted FRET assays with donor and acceptor pairs switched accordingly. VirB10 was labeled with the donor fluorophore (Alexa fluor 488) while VirB8 was labeled with the acceptor fluorophore (Alexa fluor 546). The titration curve indicated a K_D value of 0.5 μM, which is in the same range of our previous data [24] (Fig. 6A). Next, the efficiency of energy transfer was assessed in the presence of unlabeled VirB6 N-terminal peptide (Fig. 6A) and of unlabeled VirB6 central peptide (Fig. 6B). Neither of these peptides affected the energy transfer between VirB10 and VirB8 suggesting that none of the two VirB6-derived peptides affects the interaction between VirB8 and VirB10. Finally, we assessed whether there is an effect of

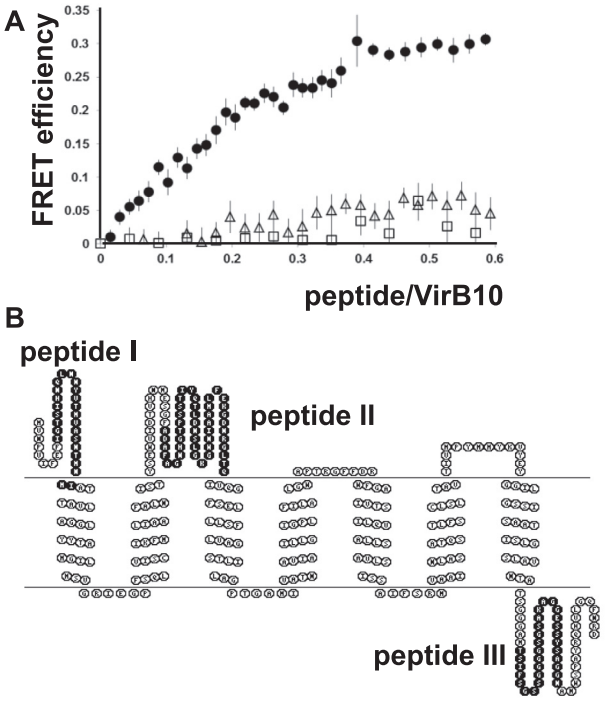

Fig. 5. Fluorescence resonance energy transfer between VirB6-derived peptides and VirB10. (A) Fluorescence emission of Alexa fluor 488 (donor) chemically attached to VirB10 (3 μM) upon increasing concentrations of VirB6-derived peptides labeled with acceptor fluorophore Alexa fluor 546 (peptide 1: filled circles, amino acids 10–33; peptide 2: empty triangles, amino acids 100–143; peptide 3: empty squares, amino acids 301–329). FRET efficiency was calculated as 1 – (F′/F) where F′ and F are the donor emission in the presence and absence of the acceptor, respectively. (B) Peptides 1–3 (amino acids in black bold print) displayed on a model of the VirB6 structure generated with TOPO2 (http://www.sacs.ucsf.edu/cgi-bin/open-topo2.py) based on the transmembrane segment prediction using TMHMM (http://www.cbs.dtu.dk/services/TMHMM/).

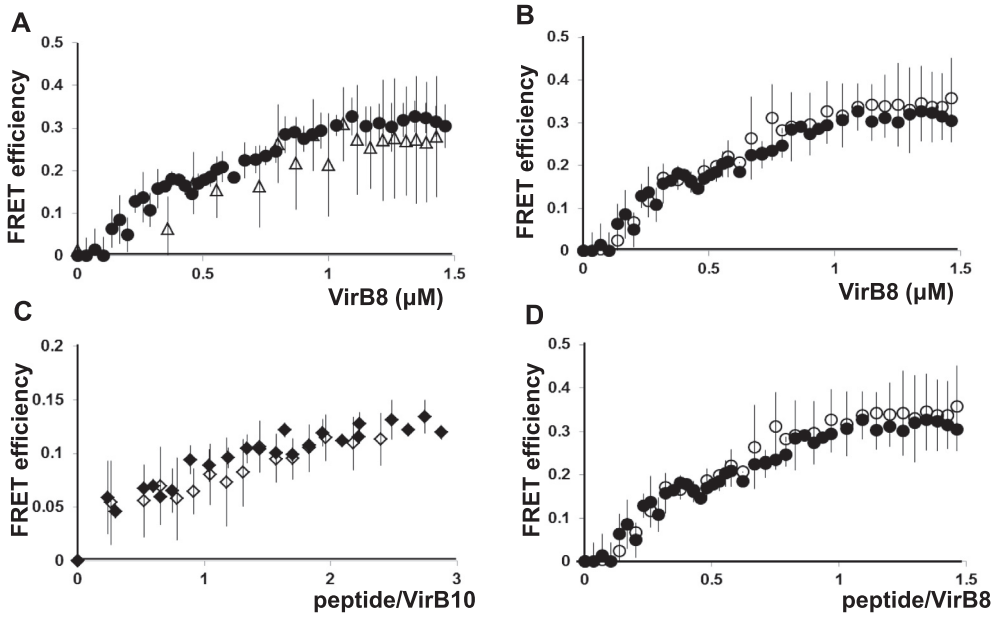

Fig. 6. Fluorescence resonance energy transfer between VirB10, VirB8 and VirB6-derived peptides. (A) Fluorescence emission of Alexa fluor 488 (donor) chemically attached to VirB10 was measured upon increasing concentrations of VirB8 labeled with Alexa fluor 546 (acceptor) in the absence (filled symbols) and presence (empty symbols) of VirB6 N-terminal peptide (amino acids 10–33) or (B) VirB8-interacting central VirB6 peptide (amino acids 100–143). (C) Fluorescence emission of Alexa fluor 488 (donor) chemically attached to VirB10 was measured upon increasing concentrations of VirB6 N-terminal peptide (amino acids 10–33) labeled with Alexa fluor 546 (acceptor) in the absence (filled symbols) or presence (empty symbols) of unlabeled wild type VirB8. (D) Fluorescence emission of Alexa fluor 488 (donor) chemically attached to VirB8 was measured upon increasing concentrations of VirB6 central peptide (amino acids 100–143) labeled with Alexa fluor 546 (acceptor) in the absence (filled symbols) or presence (empty symbols) of unlabeled wild type VirB10. FRET efficiencies were calculated as $1 - (F'/F)$ where F' and F are the donor emission in the presence and absence of the acceptor, respectively.

VirB8 (or VirB10) on the VirB6 N-terminal peptide-VirB10 (or VirB6 central peptide-VirB8) interaction. Here, the donor fluorophore was attached to VirB10 and the acceptor was attached to the VirB6 N-terminal peptide. The effects of the addition of unlabeled VirB8 were assessed. An equivalent setup was used to assess an effect of VirB10 on VirB6 central peptide-VirB8 interaction, i.e., donor-labeled VirB8, acceptor-labeled VirB6 central peptide, unlabeled VirB10. No effects were detected on the interaction of any of the proteins with the corresponding peptide from VirB6 (Fig. 6C and D). The in vitro conditions probably mimick the in vivo situation only partly, but these results suggest that VirB6 is able to interact with VirB8 and VirB10 simultaneously in a non-competitive fashion. The interactions between these three proteins are likely very important for the dynamics of T4SS assembly and our results may also help understanding the results from previous work. When the pKM101 homologs of VirB7, VirB8, VirB9 and VirB10 were overexpressed in an operon a stable complex of VirB7, VirB9 and VirB10 formed, but VirB8 did not form part of this complex [4]. On the contrary, when VirB3 to VirB10 homologs from plasmid R388 were overexpressed and purified, VirB8 formed part of the resulting complex [5]. Given that VirB6 interacts both with VirB8 and with VirB10 it could stabilize the interaction between these proteins in the natural biological context explaining the presence of VirB8 in the VirB3-VirB10 complex. This transient interaction could in turn mediate the substrate transfer from VirB6 and VirB8 to VirB9 and VirB2 for which VirB10 is absolutely required [10].

Acknowledgments

This work was supported by grants to C.B. from the Canadian Institutes of Health Research (CIHR MOP-84239), the NSERC-CREATE program on the Cellular Dynamics of Macromolecular Complexes (CDMC), the Canada Foundation for Innovation (CFI) and the Fonds de recherche du Québec-Santé (FRQ-S). We thank Peter Pawelek (Concordia University, Montreal, Canada) for the use of MATCHSCAN, Mark Smith for the construction of pHTVirB10sp and Benoit Bessette for technical assistance.

Appendix A. Supplementary data

Supplementary data associated with this article can be found, in the online version, at http://dx.doi.org/10.1016/j.febslet.2015.05.051.

References

[1] Fronzes, R., Christie, P.J. and Waksman, G. (2009) The structural biology of type IV secretion systems. Nat. Rev. Microbiol. 7, 703–714.
[2] Trokter, M., Felisberto-Rodrigues, C., Christie, P.J. and Waksman, G. (2014) Recent advances in the structural and molecular biology of type IV secretion systems. Curr. Opin. Struct. Biol. 27C, 16–23.
[3] Chandran, V., Fronzes, R., Duquerroy, S., Cronin, N., Navaza, J. and Waksman, G. (2009) Structure of the outer membrane complex of a type IV secretion system. Nature 462, 1011–1015.
[4] Fronzes, R., Schafer, E., Wang, L., Saibil, H.R., Orlova, E.V. and Waksman, G. (2009) Structure of a type IV secretion system core complex. Science 323, 266–268.
[5] Low, H.H., Gubellini, F., Rivera-Calzada, A., Braun, N., Connery, S., Dujeancourt, A., Lu, F., Redzej, A., Fronzes, R., Orlova, E.V. and Waksman, G. (2014) Structure of a type IV secretion system. Nature 508, 550–553.
[6] Cascales, E. and Christie, P.J. (2004) Definition of a bacterial type IV secretion pathway for a DNA substrate. Science 304, 1170–1173.
[7] Villamil Giraldo, A.M., Sivanesan, D., Carle, A., Paschos, A., Smith, M.A., Plesa, M., Coulton, J. and Baron, C. (2012) Type IV secretion system core component VirB8 from *Brucella* binds to the globular domain of VirB5 and to a periplasmic domain of VirB6. Biochemistry 51, 3881–3890.
[8] Jakubowski, S.J., Krishnamoorthy, V., Cascales, E. and Christie, P.J. (2004) *Agrobacterium tumefaciens* VirB6 domains direct the ordered export of a DNA substrate through a type IV secretion system. J. Mol. Biol. 341, 961–977.
[9] Karnholz, A., Hoefler, C., Odenbreit, S., Fischer, W., Hofreuter, D. and Haas, R. (2006) Functional and topological characterization of novel components of the comB DNA transformation competence system in *Helicobacter pylori*. J. Bacteriol. 188, 882–893.
[10] Cascales, E. and Christie, P.J. (2004) *Agrobacterium* VirB10, an ATP energy sensor required for type IV secretion. Proc. Natl. Acad. Sci. USA 101, 17228–17233.

[11] Maniatis, T.A., Fritsch, E.F. and Sambrook, J. (1982) Molecular Cloning: A Laboratory Manual, Cold Spring Harbor Laboratory, Cold Spring Harbor, NY.
[12] Smith, M.A., Coincon, M., Paschos, A., Jolicoeur, B., Lavallee, P., Sygusch, J. and Baron, C. (2012) Identification of the binding site of *Brucella* VirB8 interaction inhibitors. Chem. Biol. 19, 1041–1048.
[13] Hsieh, J.M., Besserer, G.M., Madej, M.G., Bui, H.Q., Kwon, S. and Abramson, J. (2010) Bridging the gap: a GFP-based strategy for overexpression and purification of membrane proteins with intra and extracellular C-termini. Protein Sci. 19, 868–880.
[14] Carter, D.M., Gagnon, J.N., Damlaj, M., Mandava, S., Makowski, L., Rodi, D.J., Pawelek, P.D. and Coulton, J.W. (2006) Phage display reveals multiple contact sites between FhuA, an outer membrane receptor of *Escherichia coli*, and TonB. J. Mol. Biol. 357, 236–251.
[15] Mandava, S., Makowski, L., Devarapalli, S., Uzubell, J. and Rodi, D.J. (2004) RELIC – a bioinformatics server for combinatorial peptide analysis and identification of protein–ligand interaction sites. Proteomics 4, 1439–1460.
[16] Laemmli, U.K. (1970) Cleavage of structural proteins during the assembly of the head of bacteriophage T4. Nature 227, 680–685.
[17] Schägger, H. and von Jagow, G. (1987) Tricine-sodium dodecyl sulfate-polyacrylamide gel electrophoresis for the separation of proteins in the range of 1 to 100kDa. Anal. Biochem. 166, 368–379.
[18] Karimova, G., Pidoux, Josette, Ullmann, Agnes and Ladant, Daniel (1998) A bacterial two-hybrid system based on a reconstituted signal transduction pathway. Proc. Natl. Acad. Sci. USA 95, 5752–5756.
[19] Wang, Z.X., Kumar, N.R. and Srivastava, D.K. (1992) A novel spectroscopic titration method for determining the dissociation constant and stoichiometry of protein-ligand complex. Anal. Biochem. 206, 376–381.
[20] Jakubowski, S.J., Kerr, J.E., Garza, I., Krishnamoorthy, V., Bayliss, R., Waksman, G. and Christie, P.J. (2009) Agrobacterium VirB10 domain requirements for type IV secretion and T pilus biogenesis. Mol. Microbiol. 71, 779–794.
[21] Nilsson, J., Persson, B. and von Heijne, G. (2000) Consensus predictions of membrane protein topology. FEBS Lett. 486, 267–269.
[22] Krogh, A., Larsson, B., von Heijne, G. and Sonnhammer, E.L. (2001) Predicting transmembrane protein topology with a hidden Markov model: application to complete genomes. J. Mol. Biol. 305, 567–580.
[23] McCafferty, J. and Schofield, D. (2015) Identification of optimal protein binders through the use of large genetically encoded display libraries. Curr. Opin. Chem. Biol. 26C, 16–24.
[24] Sivanesan, D., Hancock, M.A., Villamil Giraldo, A.M. and Baron, C. (2010) Quantitative analysis of VirB8-VirB9-VirB10 interactions provides a dynamic model of type IV secretion system core complex assembly. Biochemistry 49, 4483–4493.